Ferrielectric liquid crystal subphase studied by polarized Fourier-transform infrared spectroscopy

A. A. Sigarev,[1,2] J. K. Vij,[1,*] Yu. P. Panarin,[1] and J. W. Goodby[3]
[1]*Department of Electronic and Electrical Engineering, Trinity College, University of Dublin, Dublin 2, Ireland*
[2]*Department of Molecular Physics and Electronics, Research Institute of Physical Problems, Moscow 103460, Russia*
[3]*Department of Chemistry, University of Hull, Hull HU6 7RX, United Kingdom*
(Received 1 July 1999; revised manuscript received 11 January 2000)

IR dichroism and the structure of a homogeneously aligned cell of a chiral smectic antiferroelectric liquid crystal (R)-1-methylheptyl 4-(4′-dodecyloxybiphenyl-4-ylcarbonyloxy)-3-fluorobenzoate [with acronym (R)-12OF1M7] in a ferrielectric subphase in the temperature range between the antiferroelectric phase (also referred to as Fi2) and the smectic-*C**(SmC*) phase are studied using polarized Fourier transform IR spectroscopy. The polarization dependencies of the absorbance for several characteristic bands are quantitatively analyzed for different stages of the electrically induced structural transformations in the sample, including the helix unwinding and the phase transition from the ferriphase to the SmC* phase. A qualitative similarity of the voltage dependence of the normalized angular shift of the IR absorbance profile for the ''chiral'' carbonyl band to that of the normalized macroscopic polarization is found. The voltage dependent dichroic properties of the sample are analyzed in terms of the molecular structure and unwinding of the helical structure under an external electric field. The rotational orientational biasing of the carbonyl groups around the long molecular axis is confirmed by the spectral data. The analysis of IR dichroic data for the field induced SmC* phase is used to determine the rotational orientational distributions for the carbonyl groups.

PACS number(s): 42.70.Df, 61.30.Gd, 77.80.−e, 78.30.−j

I. INTRODUCTION

The structure and properties of ferrielectric phases which can exist in the temperature range between the antiferroelectric SmC_A^* and ferroelectric SmC* phases for chiral smectic antiferroelectric liquid crystals (AFLCs) are extensively studied and discussed [1–5]. A possible general sequence of ferri-phases can be as follows:-SmC_A^*-spr3-SmC_γ^*-spr2-AF-spr1-SmC*-, however, some of the phases may not exist in a particular AFLC material [3,5]. Designations spr1, spr2, and spr3 are related to the subphase regions in the temperature intervals between SmC* and AF, AF and SmC_γ^*, SmC_γ^*, and SmC_A^* phases, respectively.

Strictly speaking, the phase identification has to be done in the absence of an external electric field as an application of a field can destroy a delicate energy balance between ferroelectricity and antiferroelectricity and therefore some phases can disappear or arise. Recently, the existence of two ferrielectric phases labeled Fi1 and Fi2 with three-layer and four-layer periodicity of the structure, respectively, was directly confirmed at zero electric field for an AFLC material using a non-destructive technique of resonant x-ray scattering [4]. The phases Fi1 and Fi2 can be identified with the phases SmC_γ^* and AF, respectively [2,5,6].

However, for a helical structure at zero field in a cell with planar homogeneous configuration, all phases appear to be similar on analysis using a majority of techniques that are commonly used to study AFLCs. That is why an electric field is usually applied to an AFLC sample to distinguish and identify the various phases through their characteristic field dependencies of conoscopic figures, electro-optical properties, etc., with a range of techniques. Some ferrielectric subphases in regions spr1, spr2, or spr3 have been observed for a number of AFLC compounds [2,3,5], but most of them have yet not been investigated using resonant x-ray scattering. In the absence of such studies, it is desirable to investigate these phases using a variety of other techniques.

The existence of a ferrielectric subphase (labeled in Ref. [2] as a FiLC subphase) in the temperature range between AF and SmC* phases, i.e., in the subphase region spr1 for an AFLC material (R)-12OF1M7 was evidenced by conoscopic, apparent tilt angle, dielectric spectroscopy, and macroscopic polarization investigations [2]. In the present work we analyze a homogeneously aligned cell of this material in the FiLC subphase using polarized Fourier transform infrared (FTIR) spectroscopy. This technique is extremely versatile for investigating the anisotropic structures of polymers [7,8], Langmuir-Blodgett films [9], liquid crystals [10–15], and other organic materials. From the analysis of IR dichroism, the biased rotation of the carbonyl groups around the long molecular axis in ferroelectric liquid crystals (FLCs) has recently been observed [12–14]. This is an extremely important finding as this confirms the prediction made from symmetry considerations by Meyer [16] and provides the microscopic basis of the spontaneous polarization in FLCs.

In this paper we analyze the polarization dependence of the absorbance for several characteristic bands during the different stages of helix unwinding in the sample under an external electric field. We interpret the observed IR dichroic behavior in terms of the molecular structure and the molecular orientational distribution function. We also correlate the spectral results with the data on the macroscopic spontaneous polarization and the optical apparent tilt angle.

*Corresponding author. Electronic address: jvij@tcd.ie

II. EXPERIMENT

The structural formula of (*R*)-12OF1M7, synthesized in Hull, U.K., and its phase sequence determined from dielectric and macroscopic polarization measurements upon cooling [2] is as follows:

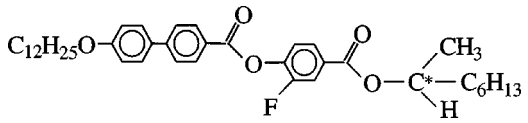

SmC_A^* (78.3 °C) SmC_γ^* (83.5 °C) AF (85 °C) FiLC (90 °C)SmC* (93 °C) SmA* (105.7 °C) Iso.

We investigate a homogeneously aligned sample of this material in the FiLC subphase. The sample was prepared between two optically polished ZnSe substrates (27 mm in diameter and 1 mm thickness) transparent to both visible and IR. The substrates were coated with a thin conducting layer of indium tin oxide (ITO) and a thin nylon 6,6 layer spin-coated over ITO electrode and then rubbed in one direction to orient the sample. The cell thickness of 6 μm was obtained using Mylar film spacers. The homogeneity of the cell thickness was confirmed by the presence of an interference pattern in the transmittance spectrum of an empty cell. The material in its isotropic phase was filled in the cell using the capillary effect. The filled cell was fitted into a special sample holder designed for optical measurements [17]. The cell temperature was held constant within an accuracy of ± 0.1 °C, using a temperature controller. The quality of alignment and the apparent tilt angle of the director in the cell were determined using optical polarizing microscopy. A chevron structure appearing in the sample after cooling from the SmA* phase to the SmC* phase was transformed to a striped-bookshelf structure by an application of a sufficiently large electric field within the SmC* phase.

The voltage dependence of the macroscopic spontaneous polarization P^* for the same cell was measured at temperatures from 80 to 90 °C using a square wave [2] of frequency 22 Hz and amplitude up to 20 V. This confirms the existence of the FiLC subphase in the sample at 85 °C. Prior to IR spectral recording, the cell was subjected to ac voltage of 1 kHz, and amplitude gradually reduced from 60 to 0 V to establish an equilibrium state of the helical structure with an optical apparent tilt angle $\sim 0°$.

Spectral measurements in the wavenumber range 650 to 4000 cm^{-1} with a resolution of 2 cm^{-1} were made using a Bio-Rad FTS-60A spectrometer equipped with a MCT detector and a wire grid polarizer. The transmission method at the normal incidence of IR radiation to the cell was used. An averaging of eight scans was used to obtain an appropriate signal-to-noise ratio greater than 500. A schematic representation of the laboratory and molecular coordinate systems is shown in Fig. 1. The angles used to describe the orientation of the molecules, transition moments and the electric vector of polarized IR radiation are explained in the caption to Fig. 1. The notations of angles, wherever possible, are similar to those adopted by Jang *et al.* [14]. Spectral measurements for the FiLC subphase at 85 °C were carried out for the dc voltage across the cell varied from 0 to 10 V with a regular step of 0.5 V. For a fixed voltage, spectra were measured for a set of angles of polarizer rotation about an axis parallel to the IR radiation propagation direction. Additional spectral measurements were made for dc voltages of 12 and 20 V of both polarities to ensure that a complete helical unwinding in the cell was achieved. To find the smectic layer normal for the SmA* phase (parallel to the rubbing direction in the cell), the polarized spectra for the sample in this phase at a temperature of 95 °C were measured at $U = 0$ V.

III. EXPERIMENTAL RESULTS

A. Macroscopic polarization vs voltage

The normalized macroscopic polarization P^*/P_S, vs applied voltage U_A for the sample at 85 °C is shown in Fig. 2. This voltage dependence of P^*/P_S for the studied sample is typical of the FiLC subphase [2]. The voltage region where P^*/P_S increases with voltage consists of three parts: two parts with almost linear increases and a final part of a non-

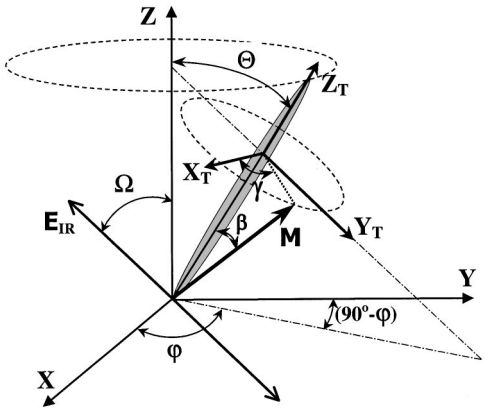

FIG. 1. The schematic of the laboratory and the molecular coordinate systems. (X,Y,Z) is the laboratory system: (Y,Z) plane is parallel to the surface of ZnSe substrates with ITO electrodes forming the cell, Z axis is parallel to the rubbing direction, X axis is along the IR radiation propagation direction; Ω is the angle between Z axis and the electric vector $\mathbf{E}_{IR}$ of polarized IR radiation. The smectic layer normal is parallel to Z axis for an ideal bookshelf structure. (X_T, Y_T, Z_T) is the molecular system: Z_T is parallel to the molecular long axis with polar angle Θ with respect to Z axis and the azimuthal angle φ; the plane (Y_T, Z_T) is parallel to the tilt plane. The transition moment $\mathbf{M}$ of a certain vibration is characterized by its polar angle β with respect to the molecular long axis and the azimuthal angle γ measured from the normal to the tilt plane.

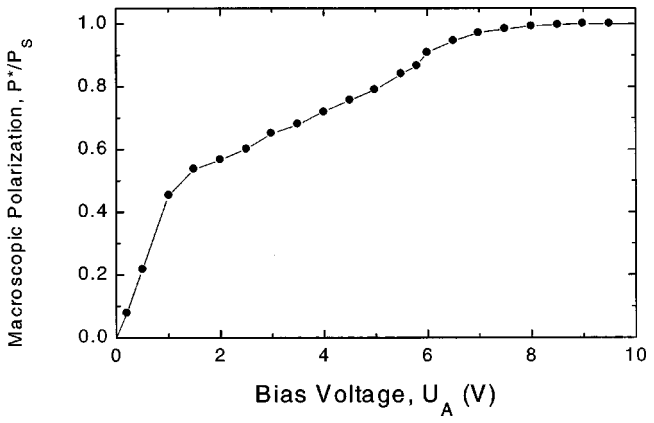

FIG. 2. Normalized macroscopic polarization, P^*/P_s, vs the bias voltage for a 6 μm cell of (R)-12OF1M7 at 85 °C. Lines interconnect adjacent points.

linear increase. For low voltages, $0\,\mathrm{V}<U_A<1.5\,\mathrm{V}$, P^*/P_S increases rapidly with voltage and reaches a value of 0.55 for $U_A=1.5\,\mathrm{V}$. This corresponds to a rapid helix distortion of the ferrielectric subphase. For higher voltages, $1.5\,\mathrm{V}<U_A<5.5\,\mathrm{V}$, a rate of increase in P^*/P_S is lower in comparison with that for lower voltages. The macroscopic polarization reaches a saturation value P_S, for $U_A\cong 8\,\mathrm{V}$, which corresponds to unwound ferroelectric SmC* phase. It is possible to suppose that with voltage increasing from ~2 to ~8 V for a 6 μm cell, an almost continuous phase transition between subphases is induced by an applied electric field.

B. Polarized IR spectra and absorbance profiles

We discuss the dichroic properties of the sample for five absorption bands given in Table I. The stretching vibrations of the C atoms of the phenyl ring, the C═O group within the core (the ''core'' carbonyl group), the C═O group attached close to the chiral center (the ''chiral'' carbonyl group), and the methylene groups are considered.

The examples of the baseline corrected polarized IR spectra in the wavenumber regions of the main interest are given in Fig. 3. The peak absorbance A defined as the difference in the absorbance at a band maximum and at a baseline level, was determined using a standard Perkin Elmer Grams Research package. For curve fitting, the Gaussian function was used to approximate the partly overlapping carbonyl bands at 1722 and 1747 cm^{-1}, the Lorentzian function was used for the other bands studied.

TABLE I. Assignment [18] for the absorption bands. Angles $\Omega_0(0\,\mathrm{V})$ and angular shifts of the absorbance profiles $\Delta\Omega_0(10\,\mathrm{V})$ for the various bands for the sample at 85 °C.

Wave number (cm^{-1})	Vibrations	$\Omega_0(0\,\mathrm{V})$	$\Delta\Omega_0(10\,\mathrm{V})$
1604	Phenyl ring C—C stretching	−0.71°	−18.72°
1722	C═O (chiral part) stretching	88.95°	−15.01°
1747	C═C (core part) stretching	−0.32°	−99.52°
2927	CH_2 asymmetric stretching	89.1°	−17.24°

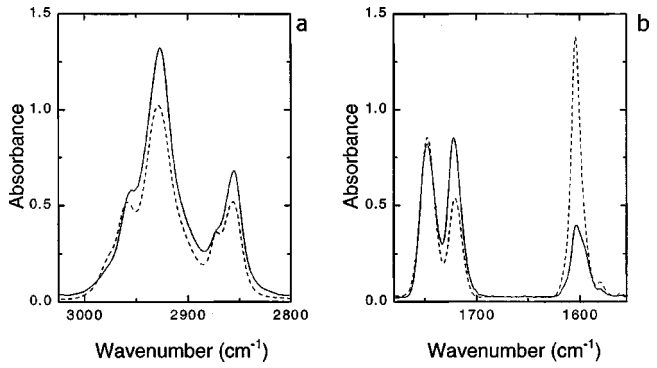

FIG. 3. Polarized spectra of a 6 μm cell of (R)-12OF1M7 (85 °C, $U=0$ V) after base line correction: (a) region of the methylene (2855, 2927 cm^{-1}) and methyl (2872, 2958 cm^{-1}) bands, (b) region of the carbonyl (1722, 1747 cm^{-1}), and phenyl (1604 cm^{-1}) bands. Electric vector of polarized IR radiation is parallel (dashed line) and perpendicular (solid line) to the rubbing direction.

Polar plots of the absorbance profiles for several bands for the equilibrium, distorted and unwound states of a helical structure are shown in Fig. 4. The polarization dependence of the absorbance for a certain band can be described by the equation [14,19,20] written in the form [19]

$$A(\Omega)=-\log_{10}[10^{-A_\parallel}+(10^{-A_\perp}-10^{-A_\parallel})\sin^2(\Omega-\Omega_0)], \tag{1}$$

Ω is the angle between the Z axis and the polarization direction of IR radiation, the angles Ω_0 and $\Omega_0+90°$ correspond to the maximal ($A_\parallel$) and minimal ($A_\perp$) values of the peak absorbance. To determine $A_\parallel$, $A_\perp$, and Ω_0 for a given absorbance profile, Eq. (1) is fitted to the experimental data. In the experiment, Ω was set to 0° for the angle of polarizer rotation for which the maximum peak absorbance for the phenyl band at 1604 cm^{-1} is observed in the SmA* phase.

The angles $\Omega_0(0\,\mathrm{V})$ for $U=0$ V and the angular shifts of the profiles for $U=10$ V are given in Table I for the various bands. The voltage dependencies of the angle Ω_0, normalized angular shift $\Delta\Omega_0(U)/\Delta\Omega_{0S}$, dichroic ratio $R=A_\parallel/A_\perp$, and absorbencies $A_\parallel$ and $A_\perp$ are shown in Figs. 5–8, respectively. The angular shift of the absorbance profile for voltage U, $\Delta\Omega_0(U)$, is defined as $\Delta\Omega_0(U)=\Omega_0(U)-\Omega_0(0\,\mathrm{V})$. For the saturated angular shift, $\Delta\Omega_{0S}$, we use $\Delta\Omega_{0S}=\Delta\Omega_0(10\,\mathrm{V})$. These IR dichroic parameters of the sample change with voltage in the range 0–9 V; no change for voltages in the range 9 to 20 V is observed. We found that a field of ~1.5 V/μm across the cell is just sufficient to unwind a helical structure.

IV. THEORETICAL CONSIDERATIONS

A. Absorbance parameters

1. A helical structure

For the model of an ideal bookshelf structure, the smectic layer normal coincides with the rubbing direction. Components of a transition moment vector **M** in the laboratory coordinate system M_X, M_Y, M_Z, can be written in terms of its

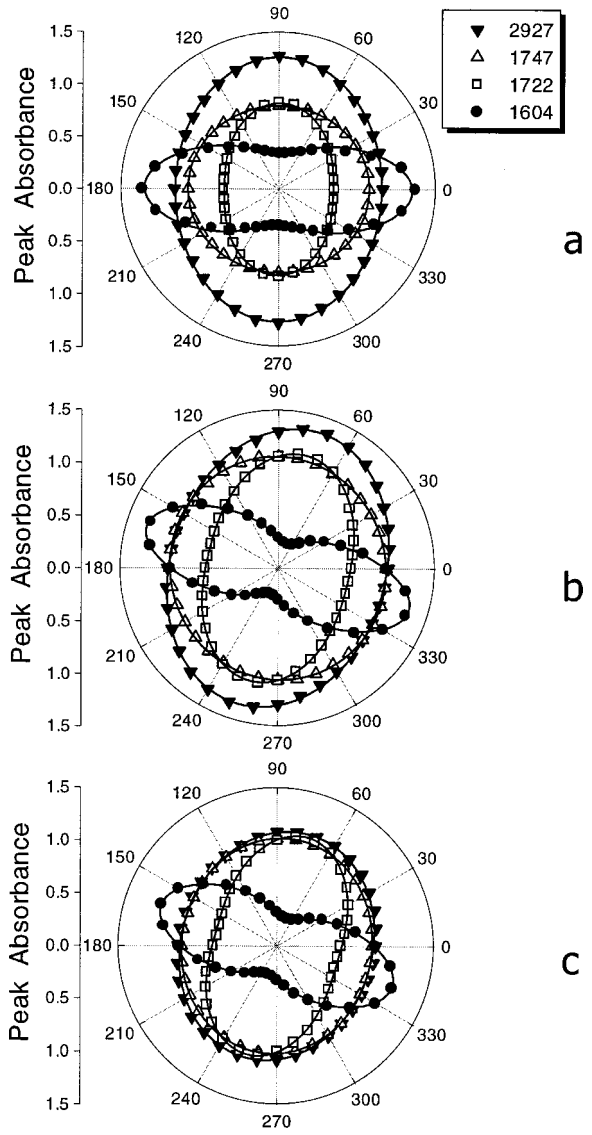

FIG. 4. The effect of dc electric field on the absorbance profiles for the phenyl (●), ''chiral'' carbonyl (□), ''core'' carbonyl (△), and methylene (▼) bands for a 6 μm cell of (R)-12OF1M7 at 85 °C. Polar plots of $A(\Omega)$ for the voltage across the cell 0 V (a), 4 V (b), 10 V (c). Signs of experimental points and wave numbers (cm^{-1}) of the respective bands are shown in insets. Curves are fits of equation (1) to experimental data.

modulus $|\mathbf{M}|$ and the angles Θ, φ, β, and γ (see Fig. 1) which describe the orientations of the molecular long axis and the transition moment as follows:

$$M_X=|\mathbf{M}|(\cos\beta\sin\Theta\cos\varphi+\sin\beta\sin\gamma\cos\Theta\cos\varphi+\sin\beta\cos\gamma\sin\varphi), \quad (2)$$

$$M_Y=|\mathbf{M}|(\cos\beta\sin\Theta\sin\varphi+\sin\beta\sin\gamma\cos\Theta\sin\varphi-\sin\beta\cos\gamma\cos\varphi), \quad (3)$$

$$M_Z=|\mathbf{M}|(\cos\beta\cos\Theta-\sin\beta\sin\gamma\sin\Theta), \quad (4)$$

For a certain absorption band, the polarization dependence of the absorbance in the (Y,Z) plane perpendicular to the IR radiation propagation direction can be expressed in terms of the following absorbances [7,14]:

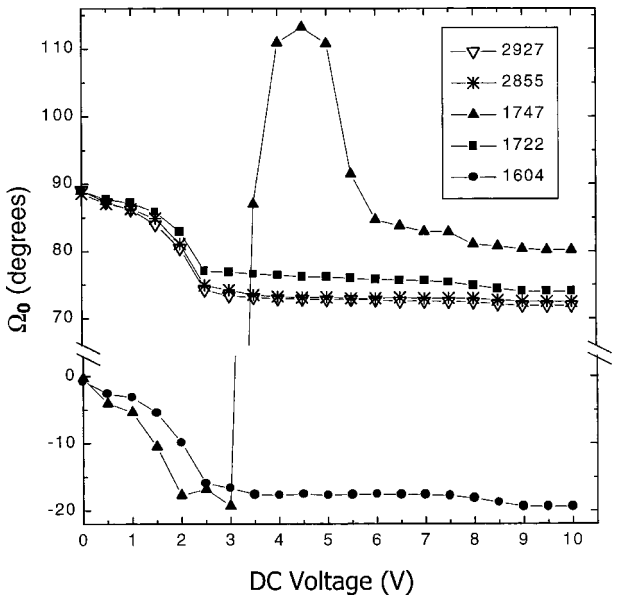

FIG. 5. Variation of the angle Ω_0 for the phenyl (●), ''chiral'' carbonyl (■), ''core'' carbonyl (▲), and methylene (*, ▽) bands with voltage for a 6 μm cell of (R)-12OF1M7 at 85 °C. Signs of experimental points and wave numbers (cm^{-1}) of respective bands are shown in the inset.

$$A_Y=k\langle M_Y M_Y\rangle,\quad A_Z=k\langle M_Z M_Z\rangle,\quad A_{YZ}=k\langle M_Y M_Z\rangle, \quad (5)$$

where the normalizing coefficient k is a constant. The absorbances (5) can be obtained by averaging over all possible orientations of the individual transition moments in the sample using formulas (2)–(4).

For a certain absorbance profile $A(\Omega)$, dichroic ratio R is defined as $R=A_{\parallel}/A_{\perp}$. Dichroic ratio $R_{Z,Y}$ is given by a ratio of the absorbances A_Z and A_Y obtained for the electric vector of polarized radiation parallel to the Z and Y axes, respectively. To calculate $R_{Z,Y}$ for the sample with an ideal helix and negligibly small molecular fluctuations in the tilt plane, the following model of molecular orientation can be used. The tilt angle Θ is constant for all the molecules, the molecules are uniformly distributed with the azimuthal angle φ. For a certain vibration, β is constant for all the molecules and the transition moments are uniformly distributed in the azimuthal angle γ. The latter corresponds to the free rotation of molecules around their long axes. For such a model the following expression [7] is derived:

$$R_{Z,Y}=\frac{A_Z}{A_Y}=\frac{4\cos^2\Theta\cos^2\beta+2\sin^2\Theta\sin^2\beta}{2\sin^2\Theta\cos^2\beta+\cos^2\Theta\sin^2\beta+\sin^2\beta}. \quad (6)$$

2. An unwound structure

We consider the field induced SmC* phase where the smectic layer structure is of bookshelf type and the helical structure is electrically unwound. We suppose the thermal fluctuations in the azimuthal angle φ (the Goldstone mode) to be suppressed. So it is possible to assume $\varphi=90°$ for all

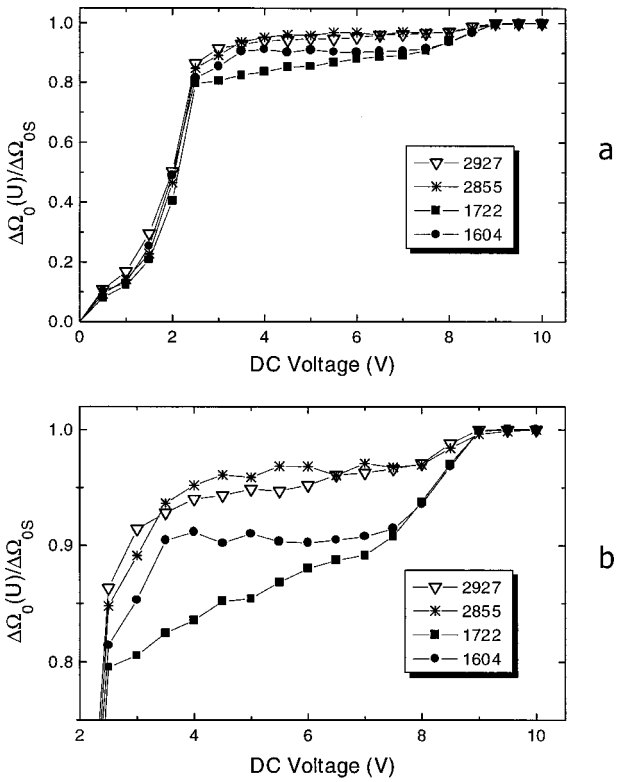

FIG. 6. (a) Normalized angular shift of the absorbance profile, $\Delta\Omega_0(U)/\Delta\Omega_{0S}$, vs applied dc voltage for the phenyl (●), ''chiral'' carbonyl (■), and methylene (*, ▽) bands. (b) A part of the plot (a) on a large scale. Sample: a 6 μm cell of (R)-12OF1M7 at 85 °C. Signs of experimental points and wave numbers (cm^{-1}) of respective bands are shown in insets.

molecules, i.e., the plane (Y_T, Z_T) coincides with the plane (Y,Z) (see Fig. 1). In this case A_Y, A_Z, and A_{YZ} can be expressed in terms of the angles Θ, β, γ using formulas (2)–(5) as in Ref. [14]:

$$A_Z = k\{\cos^2\beta\langle\cos^2\Theta\rangle - 2\sin\beta\cos\beta\langle\sin\Theta\cos\Theta\rangle\langle\sin\gamma\rangle + \sin^2\beta\langle\sin^2\Theta\rangle\langle\sin^2\gamma\rangle\}, \quad (7)$$

$$A_Y = k\{\cos^2\beta\langle\sin^2\Theta\rangle + 2\sin\beta\cos\beta\langle\sin\Theta\cos\Theta\rangle\langle\sin\gamma\rangle + \sin^2\beta\langle\cos^2\Theta\rangle\langle\sin^2\gamma\rangle\}, \quad (8)$$

$$A_{YZ} = k\{\langle\sin\Theta\cos\Theta\rangle(\cos^2\beta - \sin^2\beta\langle\sin^2\gamma\rangle) + \sin\beta\cos\beta(\langle\cos^2\Theta\rangle - \langle\sin^2\Theta\rangle)\langle\sin\gamma\rangle\}. \quad (9)$$

This analysis enables us to take into account the molecular orientational distribution in the tilt angle Θ. We consider the polar angles for the vibrational transition moments of the phenyl band β_{1604}, the ''chiral'' carbonyl band β_{1722}, and the ''core''carbonyl band β_{1747}, to have definite values for all molecules in the sample in accordance with the molecular structure.

The absorbances (5) are related to Ω_0, $A_\parallel$, and $A_\perp$ of an absorbance profile [see Eq. (1)] by the following equations [14,20]:

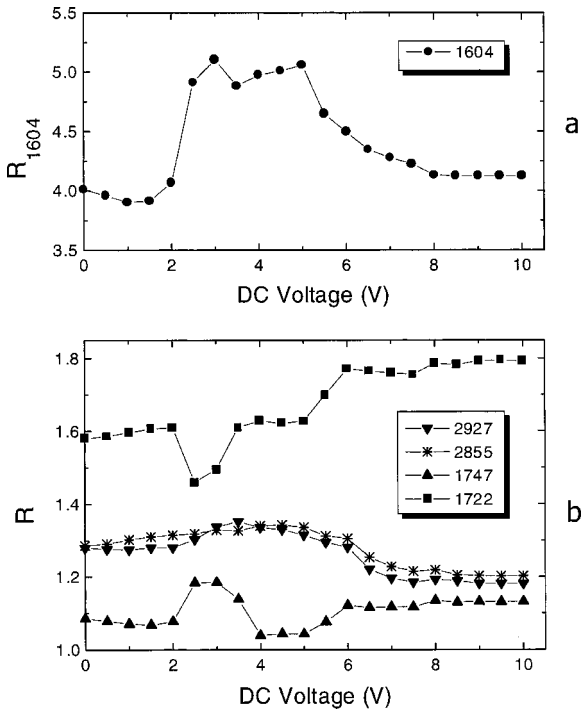

FIG. 7. Dichroic ratio, $R = A_\parallel / A_\perp$, vs applied dc voltage (a) for the phenyl band (●), (b) for the ''chiral'' carbonyl (■), ''core'' carbonyl (▲), and methylene (*, ▼) bands. Sample: a 6 μm cell of (R)-12OF1M7 at 85 °C. Signs of experimental points and wave numbers (cm^{-1}) of respective bands are shown in insets.

$$A_Y = A_\perp \cos^2\Omega_0 + A_\parallel \sin^2\Omega_0, \quad (10)$$

$$A_Z = A_\perp \sin^2\Omega_0 + A_\parallel \cos^2\Omega_0, \quad (11)$$

$$A_{YZ} = (A_\perp - A_\parallel)\sin\Omega_0\cos\Omega_0. \quad (12)$$

Azimuthal distributions of the phenyl and the carbonyl tran-

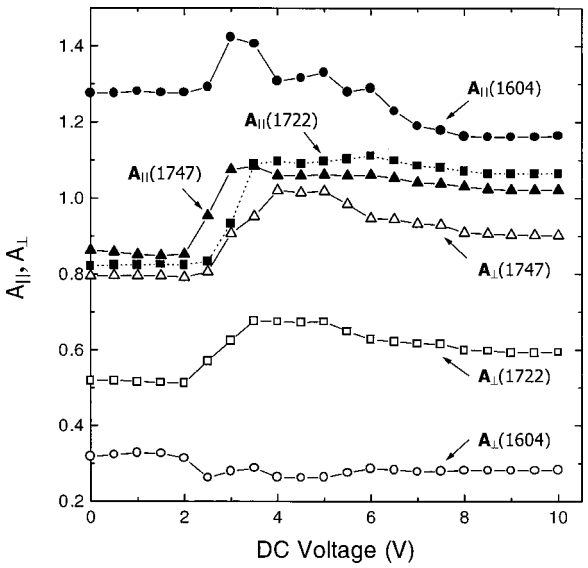

FIG. 8. Voltage dependences of $A_\parallel$ and $A_\perp$ for the phenyl (●, ○), ''chiral'' carbonyl (■, □), and ''core'' carbonyl (▼, ▽) bands at 1604, 1722, and 1747 cm^{-1}, respectively. Sample: a 6μm cell of (R)-12OF1M7 at 85 °C.

sition moments around the long molecular axis can be approximated by function $f(\gamma)$ with two Fourier components [14]

$$f(\gamma)=1/(2\pi)+a_1\cos(\gamma-\gamma_0)+a_2\cos 2(\gamma-\gamma_0), \tag{13}$$

γ_0 is the angle of biasing, coefficients a_1 and a_2 show the degree of polar and quadrupolar biasing, respectively. For $f(\gamma)$, the mean values of $\langle\sin\gamma\rangle$ and $\langle\sin^2\gamma\rangle$ used in Eqs. (6)–(8) are as follows:

$$\langle\sin\gamma\rangle=a_1\pi\sin\gamma_0,\langle\sin^2\gamma\rangle=(\tfrac{1}{2})(1-\pi a_2\cos 2\gamma_0). \tag{14}$$

As a model of an ideal unwound structure with an order parameter of unity, it is possible to consider a perfect axial orientation where the long axes of all molecules are parallel to each other and the molecules possess a rotational degree of freedom around their long axes. For a band with the polar angle β of its transition moment, the dichroic ratio R is found from the following equation [7]:

$$R=A_\parallel/A_\perp=2\cot^2\beta. \tag{15}$$

B. Molecular structure

To find β of transition moments for the various bands, the structure of the compound (R)-12OF1M7 was analyzed using a standard molecular modeling package. It is seen that the central core and the terminal alkyl chains form a bent structure of a zig-zag molecular shape typical for many chiral FLCs [21]. It is also possible to see that an ester linkage between the aromatic rings induces some bending in the core. The para-axes of the phenyl and biphenyl segments make an angle of ~10° with each other and angles of ~12°–15° with the long molecular axis (called the ''mass'' axis [21]). For the phenyl ring C—C in-plane stretching vibrations at 1604 cm^{-1}, the transition moment will lie along the para-axis of respective phenyl ring [12,22]. For simplicity, we carry out calculations in Sec. V D by considering an effective transition moment for the phenyl ring vibrations at 1604 cm^{-1} with a polar angle $\beta_{1604}=12°$.

The planes of the phenyl and biphenyl segments make an angle of ~60° with each other. The carbonyl bond of the ''chiral'' C═O group is found to be oriented in the plane of the phenyl ring and makes an angle of ~76° with respect to the long molecular axis. The ''core'' carbonyl bond lies approximately in the biphenyl plane and makes an angle of ~68° with respect to the long molecular axis. The transition moment of the C═O stretching vibrations can make an angle from 10° to 20° with the carbonyl bond [7,23]. The transition moments of the symmetric and asymmetric stretching vibrations of CH_2 groups at 2855 and 2927 cm^{-1}, respectively, are almost normal to the axis of an aliphatic chain [7].

V. DISCUSSION

A. $\Delta\Omega_0$ vs dc voltage for the phenyl, ''chiral'' carbonyl, and methylene bands

For the initial helical and final unwound structures, the orientations of the absorbance profiles for all bands, except the ''core'' carbonyl band, are typical of FLCs [12–14]. For $U=0$ V, we obtain $\Omega_0\cong 0°$ for the phenyl band. This implies that the large axis of the phenyl profile is almost parallel to the rubbing direction [see Fig. 4(a)]. For the ''chiral'' carbonyl band and both methylene bands, $\Omega_0\cong 90°$. The results for the ''core'' carbonyl band are discussed in Sec. V B.

For an unwound structure at $U=10$ V, the phenyl profile is rotated by a molecular apparent tilt angle of ~19°. This angle is close to the optical tilt angle ~20°, determined using polarizing microscopy. The large axes of the profiles for the bands at 1604, 1722, 2855, and 2927 cm^{-1} are rotated in the same direction, the sense of which is dependent on the polarity of the dc voltage. The angular shifts of these profiles achieve saturated values in the range of ~15°–19°, depending on the band, for a voltage of ~9 V [see Figs. 4(c), 5, and Table II]. The observed asymmetry of the profiles for the carbonyl and methylene bands with respect to the major axis of the phenyl profile is a consequence of the biased rotation of molecules around their long axes [12].

Three characteristic regions with considerably different rates of increase in $\Delta\Omega_0/\Delta\Omega_{0S}$ with voltage are seen in Fig. 6. For the region $0<U<2.5$ V, a rapid increase in $\Delta\Omega_0/\Delta\Omega_{0S}$ with voltage is observed for the various bands. This corresponds to a rapid deformation of a ferroelectric helix under increasing external electric field. For the bands exhibiting higher dichroism (1604, 1722, 2855, and 2927 cm^{-1}), the values of $\Delta\Omega_0(U)/\Delta\Omega_{0S}$ are approximately the same. For $U=2.5$ V, the angular shifts are about 80–85 % of the respective maximum values $\Delta\Omega_{0S}$.

There are however some differences for these bands in the higher voltage region [see Fig. 6(b)]. For the phenyl and the two methylene bands, there is an increase in $\Delta\Omega_0(U)/\Delta\Omega_{0S}$ with voltage in the range 2.5–3.5 V followed by almost a constant dependence in the range 3.5–7.5 V. But for the ''chiral'' C═0 band, the angular shift of the profile exhibits almost linear increase with voltage in the range 2.5 to 7.5 V. The rate of the angular shift increase for this range is considerably lower than for the range 0–2.5 V. For a range of 7.5–9 V, a somewhat higher rate of increase in $\Delta\Omega_0(U)/\Delta\Omega_{0S}$ with voltage, than for 2.5–7.5 V, is observed for all absorption bands.

It is important to note that the voltage dependence of $\Delta\Omega_0/\Delta\Omega_{0S}$ for the band at 1722 cm^{-1} is qualitatively similar to that of P^*/P_S given in Fig. 2. Both plots consist of three parts with considerably different slopes. These parts correspond to different stages and rates of change of the molecular orientational distribution function due to the field induced helix unwinding. The observed similarity can arise from the head-and-tail equivalence of the molecules in the FLC sample, the properties of the molecular orientational distribution and the molecular structure. In particular, the orientations of the vibrational transition moment and the dipole moment of the ''chiral'' C═O group in a molecule are of great importance. This result confirms that the macroscopic spontaneous polarization in the sample is caused mainly by the orientational ordering of the ''chiral'' C═O groups.

These results and the previous results on dielectric response [2] show that for the FiLC subphase, the electrically induced rapid angular shift of the IR absorbance profiles for the various bands with voltage in the low voltage range cor-

responds to a rapid distortion of a ferroelectric helix. The following slow angular shift of the profiles with voltage corresponds presumably to an almost continuous phase transition to the field induced SmC* phase through some intermediate subphases.

B. Dichroic behavior of the ''core'' carbonyl band

The band at 1747 cm^{-1} has unusual dichroic properties different from those of the other bands considered. This band possesses low dichroism, $1<R_{1747}<1.2$ (Fig. 7). Hence the polar plot of its absorbance profile is close to a circle (Fig. 4). The dependence of Ω_0 on voltage for this band is unique (see Fig. 5). For helical and distorted helical structures at voltages in the range 0 to 3 V, the angle Ω_0 for this band does not differ significantly from that for the phenyl band. But for a strongly distorted helix, a voltage increase from 3 to 3.5 V causes an abrupt change in Ω_0 for this band. For $U>6$ V, the polarization direction corresponding to maximum absorbance for this band is approximately perpendicular to that for $U=0$ V.

The dichroic behavior of the ''core'' carbonyl band shows that β_{1747} is close to a critical value of the polar angle of 54.44°, for which the dichroic ratio is equal to 1 for the models of both the helical [Eq. (6)] and unwound structures [Eq. (15)]. This conclusion is supported by the results to be discussed in Sec. V D.

C. *R* vs dc voltage

The dependencies of R, $A_\parallel$, and $A_\perp$ on dc voltage for the various bands are shown in Figs. 7 and 8. R for the phenyl band, R_{1604}, changes in the range 4 to 5 and is 3 to 4 times higher than for the other four bands. Such a difference in R for the various bands is connected with the difference in the polar angles β of the respective transition moments. Since the transition moment of the phenyl ring C-C vibration at 1604 cm^{-1} is approximately parallel to the long molecular axis, it is possible to consider Ω_0 and R_{1604} for the phenyl band as the parameters characterizing the direction and the degree of preferable orientation of molecules, respectively.

Experimental values of R_{1604} for the sample are found to be considerably lower than estimated using Eqs. (6) and (15) for $\Theta=20°$ and $\beta_{1604}=15°$ for both the helical and the unwound states. This discrepancy shows that the order parameter is less than 1. Figure 7 shows marked different dependencies of R_{1604} on voltage for five voltage regions. In region 1 ($0\ V<U<2\ V$), rather small changes in R, $A_\parallel$, and $A_\perp$ are observed for all bands. In region 2 ($2\ V<U<2.5\ V$), R_{1604} and R_{1747} increase by 25 and 10 %, respectively, whereas R_{1722} shows a 10% decrease. The increase in R_{1604} occurs mainly due to a decrease in $A_\perp$ whereas an increase in $A_\parallel$ is relatively small (Fig. 8). In region 3 ($2.5\ V<U<5\ V$), R_{1604} is maximal and displays a small gradual increase in the 3.5 to 5 V range. In this region, R_{1722} and R_{1747} display variations opposite to those observed for these bands in region 2.

Several effects accompanying the helix distortion can contribute to a change in R_{1604}. Preferable orientating of the molecules parallel to substrates at a certain tilt angle with the smectic layer normal causes an increase in R_{1604}. The presence of the substrate-adjacent layers with preferable orientation of the molecules remaining along the rubbing direction [24,25] contributes to a decrease in R_{1604}. The structure transformation from ferrielectric to ferroelectric phase can also influence R_{1604}.

From results for regions 1–3 (Fig. 7), we conclude that the electrically induced distortion of the helical structure is accompanied with marked and discontinuous changes in R, $A_\parallel$, $A_\perp$, and Ω_0 for the phenyl and two carbonyl bands. For the methylene bands, however, changes in R are not so pronounced. This shows that the degree of ordering for the hydrocarbon tails is lower than for the molecular long axes because of a bent molecular shape.

Results for region 4 ($5\ V<U<8\ V$), are quite interesting. For a given sample, $U\cong 5$ V is considered to be a threshold voltage exceeding which, a gradual decrease in R_{1604} with voltage is observed. This is accompanied with both a decrease in $A_\parallel$ and an increase in $A_\perp$. A lower decrease in R with voltage occurs for the methylene bands. On the contrary, for both carbonyl bands, a resultant increase in R with voltage is observed. Saturated values of R, $A_\parallel$, and $A_\perp$ are reached for $U\cong 8$ V for the various bands. In particular, R_{1722} is maximal for $U>8$ V. It means that the degree of preferable orientation of the ''chiral'' C═O groups in the sample is maximum for the electrically unwound helix due to the polar interactions of C═O dipole moments with external electric field. It is important to note that there is no change in Ω_0 for the phenyl band for the region 5–7.5 V (Fig. 6). It means that the direction of preferable orientation of the molecules in the (Y,Z) plane remains the same but the degree of molecular ordering decreases. In region 5 ($8\ V<U<10\ V$), values of R, $A_\parallel$, and $A_\perp$ remains constant for all bands.

We explain that a decrease in R_{1604} for the range 5 to 8 V is due to an electrically induced increase in the area for horizontal chevron structure at the expense of the area for vertical chevron structure within the stripes in the sample as described in Ref. [26]. A ferroelectric liquid crystal cell with a striped texture contains areas of both chevron and bookshelf within the stripes (zig-zag walls) and an application of reasonable dc voltage to a cell can induce a change in the layer structure from vertical chevron to horizontal chevron [26]. Using a polarizing microscope, we observed the appearance of more distinct stripe texture in form of defect lines parallel to the rubbing direction for $U>8$ V, compared to that for $U<5$ V. These are presumably caused by such structural transformation.

The decrease in R_{1604} due to the transformation of the layer structure from vertical chevron to striped bookshelf (horizontal chevron) is explained in Fig. 9. For an unwound structure, we consider all molecules to lie parallel to the substrate surface. For the vertical chevron structure [Figs. 9(a) and 9(b)], the layers are tilted with respect to the substrates, the molecules make a switching angle $\alpha<\Theta_0$ (Θ_0 is the molecular tilt angle in a smectic layer) with Z axis, in accordance with the orientation of the respective FLC cones. On average, the molecules are parallel to each other and this results in the maximal value of R_{1604}. For the striped-bookshelf structure [Figs. 9(c) and 9(d)] the smectic layers are normal to the substrates and undulated in the (Y,Z) plane. The smectic layer normal is turned alternatively with respect to the rubbing direction by an angle of $-\Psi$ or $+\Psi$ for C and

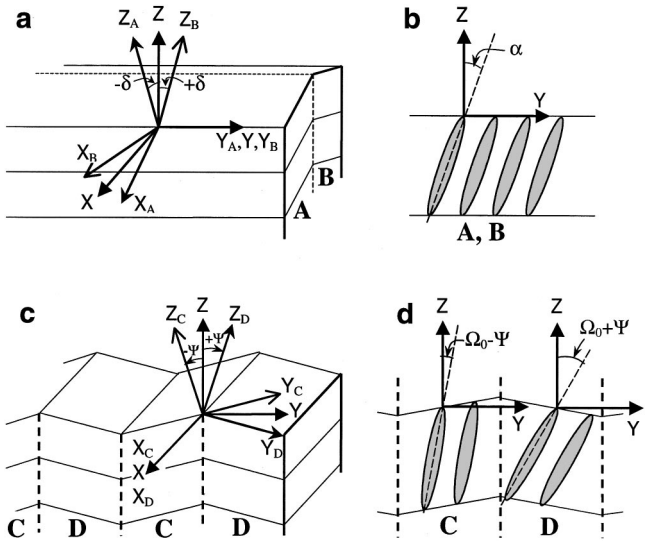

FIG. 9. A schematic illustration of the smectic layer structure for chevron (a) and striped-bookshelf (b) in the coordinate system (X,Y,Z) related to the cell: X axis is normal to the substrates, Z axis is parallel to the rubbing direction. The coordinate systems (X_A,Y_A,Z_A) and (X_B,Y_B,Z_B) are related to the parts A and B of the chevron structure, respectively, (a): Z_A and Z_B axes are the layer normal for the parts A and B, respectively, Y_A and Y_B axes are parallel to Y axis. The coordinate systems (X_C,Y_C,Z_C) and (X_D,Y_D,Z_D) are related to the parts C and D of a stripe, respectively (c): Z_C and Z_D axes are the layer normal for the parts C and D, respectively, X_C and X_D axes are parallel to the X axis. A preferable orientation of the molecules in the (Y,Z) plane for an electrically unwound helical structure $(+U)$ for chevron (b) and striped-bookshelf (d). The angles α, δ, Θ_0, and Ψ are described in the text.

D parts of a stripe, respectively. As found [26,27], $\Psi \cong \delta = k_1\Theta_0$, where δ is the smectic layer tilt angle for the chevron geometry and k_1 is a constant less than 1. This gives an angle 2Ψ between the directors for the molecules in adjacent parts of a stripe. For $\Psi \neq 0$, R_{1604} will be lower than for the vertical chevron structure.

For a striped-bookshelf structure, a resultant profile $A(\Omega)$ with parameters Ω_0 and R_{1604} can be represented by equation $A(\Omega)=(1/2)\{A_C(\Omega)+A_D(\Omega)\}$ in terms of the phenyl profiles $A_C(\Omega)$ and $A_D(\Omega)$ for the bookshelf structure parts C and D of a stripe, respectively [Figs. 9(c) and 9(d)]. For the profiles $A_C(\Omega)$ and $A_D(\Omega)$, the maximal values of the absorbance correspond to the polarization angles $\Omega_0-\Psi$ and $\Omega_0+\Psi$, respectively, and the dichroic ratio may be considerably higher than for the resultant profile $A(\Omega)$, depending on Ψ. This model explains both a decrease in $A_\parallel$ and an increase in $A_\perp$ and a resultant decrease in R_{1604} with small changes in Ω_0 for the phenyl band, for an electrically induced transformation from chevron to striped bookshelf or a horizontal chevron within the stripes.

D. Rotational distribution function $f(\gamma)$

We find the parameters for the azimuthal distribution (13) of the C═O transition moments from the experimental spectral data for the unwound helical structure. For the phenyl and two carbonyl bands, we consider two dichroic ratios $R_{Y,Z}=A_Y/A_Z$ and A_{YZ}/A_Z, expressed as functions of the angles Θ, β, and γ using Eqs. (7)–(9). Note that these equations can also be used for a striped-bookshelf geometry since the molecular tilt planes are parallel to the (Y,Z) plane for both parts of a stripe. The molecular orientational distribution in the angle Θ due to the tilt of the smectic layer normal with respect to the rubbing direction by angles $+\Psi$ or $-\Psi$ and due to the thermal fluctuations in the tilt plane is taken into account in terms of $\langle\cos^2\Theta\rangle$ and $\langle\sin\Theta\cos\Theta\rangle$. The angular biasing parameters γ_0 for the various bands are assumed to be dependent on the molecular structure of the material. Since the molecular core is sufficiently rigid, the coefficients a_1 and a_2 characterizing the degree of biasing are taken to be the same for the vibrations being considered. In the fitting procedures we use numerical values for A_Y/A_Z and A_{YZ}/A_Z obtained from experimental data through Eqs. (10)–(12), on using Ω_0, $A_\parallel$, and $A_\perp$ for the respective bands for $U=10$ V.

TABLE II. Parameters of C═O vibrational transition moments for the ''chiral'' (1722 cm^{-1}) and ''core'' (1747 cm^{-1}) carbonyl bands in the electric field induced SmC* phase at 85 °C.

β_{1604}	Carbonyl band	$\beta_{C=O}$	$\langle\sin\gamma\rangle$	$\langle\sin^2\gamma\rangle$	a_1	a_2	γ_0
0°	1722 cm^{-1}	66.8°	0.0436	0.499	0.02	0.01	43.8°
0°	1747 cm^{-1}	57.6°	0.0234	0.488	0.02	0.01	21.8°
12°	1722 cm^{-1}	66.2°	0.0361	0.503	0.015	0.009	51.8°
12°	1747 cm^{-1}	57.4°	0.0215	0.49	0.015	0.009	27.9°

The procedure developed in Refs. [14,15] for obtaining the rotational distributions for C═O groups includes the determination of a coefficient k used in Eqs. (7)–(9) from the spectral data for the SmA* phase. The analysis of ratios A_Y/A_Z and A_{YZ}/A_Z enables us to eliminate k and therefore the spectral data for the SmA* phase is not required. This approach is substantiated since the values of β for the SmA* phase may be different from those for a tilted phase due to a possible dependence of the molecular conformation on temperature [28].

To a first approximation, β_{1604} is taken to be zero. The initial values for β_{1722} and β_{1747} are obtained from the experimental data for the two carbonyl bands using Eqs. (7)–(12) and on assuming a negligible quadrupolar biasing. The latter means $a_2=0$ in relations (13) and (14). Values for $\langle\cos^2\Theta\rangle$ and $\langle\sin\Theta\cos\Theta\rangle$ are determined from A_Y/A_Z and A_{YZ}/A_Z for the phenyl band using Eqs. (7)–(12). The values $\beta_{1722}=66.8°$ and $\beta_{1747}=57.3°$ determined from this analysis are reasonably close to 60°, a polar angle of a carbonyl bond with respect to adjacent phenyl ring reported for several ether compounds [14]. Then, β, γ_0, a_1, a_2 for the carbonyl vibrations are varied to fit functions A_Y/A_Z and A_{YZ}/A_Z expressed through Eqs. (7)–(9) to the numerical values obtained from the experimental data using Eqs. (10)–(12). The results are given in Table II for $\beta_{1604}=0°$.

We also determine the biasing parameters for C═O transition moments using an approximate value $\beta_{1604}=12°$ obtained from an analysis of the molecular structure. During the fitting procedure of ratios A_Y/A_Z and A_{YZ}/A_Z of the carbonyl bands, we use almost the same values for $\langle\cos^2\Theta\rangle$ and $\langle\sin\Theta\cos\Theta\rangle$ as used in the fitting procedure for $\beta_{1604}=0°$. Values for these parameters are optimized using Eqs.

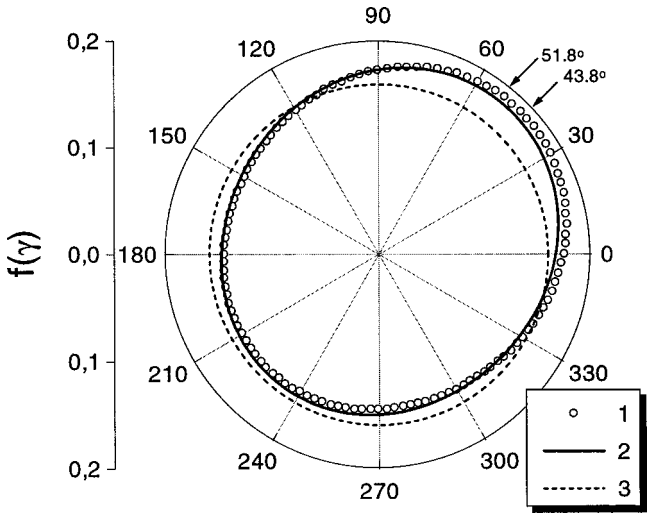

FIG. 10. Possible rotational distributions $f(\gamma)$ of the transition moment of C═O (chiral part) stretching vibrations at 1722 cm^{-1} for the 12OF1M7 sample in the electric field induced SmC* phase at 85 °C. The curve of circles (1) and the solid curve (2) show $f(\gamma)$ in a polar plot for the models of $\beta_{Ph}=0°$ and $\beta_{Ph}=12°$, respectively, for the molecules with the ''chiral'' C_8H_{17} tail oriented toward the reader. For comparison, the function $f(\gamma)=1/(2\pi)$ for the free rotation of a transition moment $[a_1=a_2=0$ in Eq. (13)] is shown by the dashed curve (3).

(7)–(12) for the phenyl band, taking into account the biasing parameters obtained for both carbonyl bands in the previous case ($\beta_{1604}=0°$) and the analysis of torsion angles for various segments of the molecular core. The results are shown in Table II for $\beta_{1604}=12°$.

The values $\beta_{1722}=66.2°\pm0.6°$ and $\beta_{1747}=57.4°\pm0.2°$ found from the fitting procedure are approximately 10° lower than the polar angles of the respective C═O bonds in a molecule. This agrees with a reported angle between the transition moment and the chemical bond for a carbonyl group [7,23]. Note that the determined β_{1747} is ~3° higher than a critical polar angle for which dichroic ratio is unity in Eqs. (6) and (15). This agrees with the results of the dichroic behavior of the ''core'' C═O band reported in Sec. III D.

Figure 10 shows $f(\gamma)$ for the transition moment of the ''chiral'' carbonyl band for the fitting parameters from Table II. For the approximations used, $\beta_{1604}=0°$ and $\beta_{1604}=12°$, two distributions $f(\gamma)$ are found to be close to each other though the most probable biasing angles γ_0 are slightly different. Approximately the same rotational distribution function (shifted by an azimuthal angle less than 20°) can be expected for the directions of the ''chiral'' C═O bonds.

On following the analysis developed in Refs. [12,14] it is possible to show that the biasing in rotation of molecules around their long axes satisfactorily explains the appearance of the spontaneous polarization along the C_2 symmetry axis in the SmC* phase due to the head-and-tail equivalence of the molecules. It is important to note that for the striped-bookshelf geometry with the electrically unwound structure, the C_2 axes for both parts of a stripe are parallel to each other and are along the normal to the substrate, that is along the external electric field. Low values of the parameters a_1 and a_2 for (R)-12OBP1M7 reflect lower value of the macroscopic spontaneous polarization in the electrically induced SmC* phase compared to materials studied in Refs. [14,15].

VI. CONCLUSIONS

From the analysis of polarized IR spectra, the following conclusions are drawn. The voltage dependence of the angular shift of the absorbance profile for the ''chiral'' C═O band is found to be qualitatively similar to that of the macroscopic spontaneous polarization. The rate of the angular shift of the profiles for the various bands with voltage reflects the rate of change of the molecular orientational distribution function during the helix unwinding under electric field. An initial rapid angular shift of the profiles shows a rapid distortion of a helix for the ferrielectric FiLC subphase. The following slow process of the angular shift of the profiles corresponds presumably to an almost continuous phase transition to the field induced SmC* phase through some intermediate subphases.

Voltage dependent dichroic properties of the various absorption bands are closely connected with both the polar angle of the respective transition moments with the molecular long axis and the structure of the sample. The analysis of dichroic ratios A_Y/A_Z and A_{YZ}/A_Z for the phenyl and carbonyl bands is used to find the orientational distribution function and the polar angle β for the C═O transition moments for the field induced SmC* phase. The biased rotational motion of molecules around their long axes is confirmed. The values of β for the ''chiral'' and the ''core'' carbonyl bands are found to be $66.2°\pm0.6°$ and $57.4°\pm0.2°$, respectively.

ACKNOWLEDGMENTS

The work was partly funded by the EU Grant ORCHIS. A.A.S. was partly supported by the Provost Academic Development Fund. We thank A. Kocot and M. Hird for discussions and O. E. Kalinovskaya for the macroscopic polarization measurements.

[1] T. Isozaki, H. Takezoe, A. Fukuda, Y. Suzuki, and I. Kawamura, J. Mater. Chem. **4**, 237 (1994).

[2] Yu. P. Panarin, O. Kalinovskaya, J. K. Vij, and J. W. Goodby, Phys. Rev. E **55**, 4345 (1997).

[3] K. Itoh, M. Kabe, K. Miyachi, Y. Takanishi, K. Ishikawa, H. Takezoe, and A. Fukuda, J. Mater. Chem. **7**, 407 (1997).

[4] P. Mach, R. Pindak, A.-M. Levelut, P. Barois, H. T. Nguyen, C. C. Huang, and L. Furenlid, Phys. Rev. Lett. **81**, 1015 (1998).

[5] T. Matsumoto, A. Fukuda, M. Johno, Y. Motoyama, T. Yui, S. S. Seomun, and M. Yamashita, J. Mater. Chem. **9**, 2051 (1999).

[6] H. T. Nguyen, J. C. Couillon, P. Cluzeau, G. Sigaud, C. Destrade, and N. Isaert, Liq. Cryst. **17**, 571 (1994).

[7] R. Zbinden, *Infrared Spectroscopy of High Polymers* (Academic, New York, 1964).

[8] D. I. Bower and W. F. Maddams, *The Vibrational Spectroscopy of Polymers* (Cambridge University Press, Cambridge, UK, 1989).
[9] P.-A. Chollet, Thin Solid Films **68**, 13 (1980).
[10] A. Kocot, G. Kruk, R. Wrzalik, and J. K. Vij, Liq. Cryst. **12**, 1005 (1992).
[11] E. Hild, A. Kocot, J. K. Vij, and R. Zentel, Liq. Cryst. **16**, 783 (1994).
[12] K. H. Kim, K. Ishikawa, H. Takezoe, and A. Fukuda, Phys. Rev. E **51**, 2166 (1995).
[13] K. Miyachi, J. Matsushima, Y. Takanishi, K. Ishikawa, H. Takezoe, and A. Fukuda, Phys. Rev. E **52**, R2153 (1995).
[14] W. G. Jang, C. S. Park, J. E. Maclennan, K. H. Kim, and N. Clark, Ferroelectrics **180**, 213 (1996).
[15] A. Kocot, R. Wrzalik, B. Orgasinska, T. Perova, J. K. Vij, and H. T. Nguyen, Phys. Rev. E **59**, 551 (1999).
[16] R. B. Meyer, Liq. Cryst. **40**, 33 (1977).
[17] T. S. Perova, A. Kocot, and J. K. Vij, Supramol. Sci. **4**, 1 (1997).
[18] L. J. Bellamy, *The Infrared Spectra of Complex Molecules* (Methuen & Co., London, 1954).
[19] A. Kocot, R. Wrzalik, and J. K. Vij, Liq. Cryst. **21**, 147 (1996).
[20] N. A. Clark (private communication).
[21] J. W. Goodby, in *Ferroelectric Liquid Crystals: Principles, Properties and Applications*, edited by J. W. Goodby *et al.* (Gordon and Breach Science Publishers, Philadelphia, 1991), Vol. 7, p. 99.
[22] L. M. Sverdlov, M. A. Kovner, and E. P. Krainov, *Vibrational Spectra of Polyatomic Molecules* (Israel Program in Science Translation, Jerusalem, 1974).
[23] K. Abe, K. Yanagisawa, J. Polym. Sci. **36**, 536 (1959).
[24] L. M. Blinov, V. G. Chigrinov, *Electro-optic Effects in Liquid Crystal Materials* (Springer-Verlag, New York, 1994).
[25] A. A. Sonin, *The Surface Physics of Liquid Crystals* (OPA, Amsterdam, 1995).
[26] R. F. Shao, P. C. Willis, and N. A. Clark, Ferroelectrics **121**, 127 (1991).
[27] Yu. P. Panarin, Yu. P. Kalmykov, S. T. Mac Lughadha, H. Xu, and J. K. Vij, Phys. Rev. E **50**, 4763 (1994).
[28] H. F. Gleeson, L. Baylis, W. K. Robinson, J. T. Mills, J. W. Goodby, A. Seed, M. Hird, P. Styring, C. Rosenblatt, and S. Zhang, Liq. Cryst. **26**, 1415 (1999).